Article

Tailoring Tautomerization of Single Phthalocyanine Molecules through Modification of Chromophore Photophysics by the Purcell Effect of an Optical Microcavity

Wassie Mersha Takele, Frank Wackenhut,* Quan Liu, Lukasz Piatkowski,* Jacek Waluk, and Alfred J. Meixner*

ACCESS | 📊 Metrics & More | 📖 Article Recommendations | 🔵 Supporting Information

ABSTRACT: Over the years, probing and controlling tautomerization has attracted significant attention because of its fundamental importance in various chemical and biological phenomena. So far, light, force, electrons, and electric field have been employed to alter the tautomerization characteristics in porphyrin and phthalocyanine derivatives. Here, we show that engineering the photophysics of molecules through interaction with the vacuum electromagnetic field in an optical microcavity can be used to control the tautomerization of single phthalocyanine molecules. Compared to the molecules embedded in a polymer matrix in open space, the average fluorescence lifetime inside the resonant microcavity decreases significantly due to the Purcell effect. The decreased lifetime reduces the possibility of a molecule entering into the triplet state, i.e., the photoactive tautomerization channel. As a result, the photoinduced tautomerization in phthalocyanine can be significantly altered. Our results demonstrate that the weak coupling between the excited state of a molecule and the vacuum electromagnetic field via a cavity mode can lead to significant changes in photoreactivity.
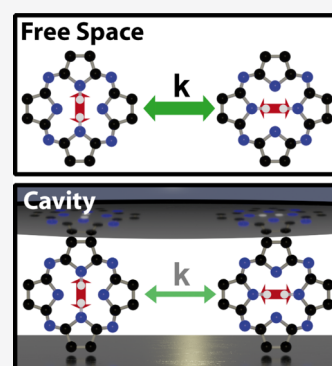
INTRODUCTION

Probing[1−7] and controlling[8−14] tautomerization has attracted significant research attention due to its fundamental importance in many biological[15] and chemical processes.[16] Within porphyrin[17,18] and phthalocyanine[19,20] derivatives, NH tautomerization occurs when the two inner hydrogen atoms migrate in the framework of the cavity consisting of four nitrogen atoms. NMR techniques[1,21] have been widely used to investigate the ground-state tautomerization processes of molecular ensembles, while pump−probe polarization spectroscopy has enabled the detection of both the ground- and excited-state proton-transfer rates.[22] Low-temperature scanning tunneling microscopy (STM) has allowed manipulation of tautomerization by additional external stimuli such as light,[10] force,[11] or current.[12,13] For instance, Ladenthin et al.[11] showed that cis ↔ cis tautomerization in a single porphycene molecule on a Cu(110) surface at 5 K could be triggered via an external force, by bringing a metallic tip close to a molecule at a zero bias voltage. Liljeroth et al.[13] demonstrated that a voltage pulse at the STM tip could induce switching of tautomerization in single naphthalocyanine molecules adsorbed on ultrathin insulating films at low temperature. Most recently, Mangel et al.[14] have also controlled the intramolecular proton-transfer reaction in phthalocyanine molecules by lowering the tautomerization barrier with a static electric field. However, an optical microcavity allows to influence the photophysical properties without modifying the local environment or the molecular structure but altering the

excited state lifetime due to the Purcell effect, an alteration of the spontaneous emission rate by modifying the local density of optical states (LDOSs).[23] Consequently, a change of the excited state lifetime could also modify photoinduced reactions, which has up to now only been achieved for strongly coupled systems. The Purcell effect has been used to suppress photobleaching,[24] enhance fluorescence emission,[25] control Förster resonance energy transfer,[26,27] and reduce the blinking behavior of individual fluorophores in the vicinity of a metal surface.[28]

In this work, we control the tautomerization of single phthalocyanine molecules by modifying the optical mode density with a $\lambda/2$ Fabry−Pérot microcavity. Phthalocyanine derivatives (Pcs) have intense Q-bands in their absorption spectra[29] and large fluorescence quantum yields compared to porphyrins.[30] These properties make Pcs a good choice for single-molecule spectroscopy studies. For instance, Yang et al.[31] used zinc Pc molecules to achieve a sub-nanometer resolution in single-molecule photoluminescence imaging. Similarly, porphyrin derivatives have been used to observe
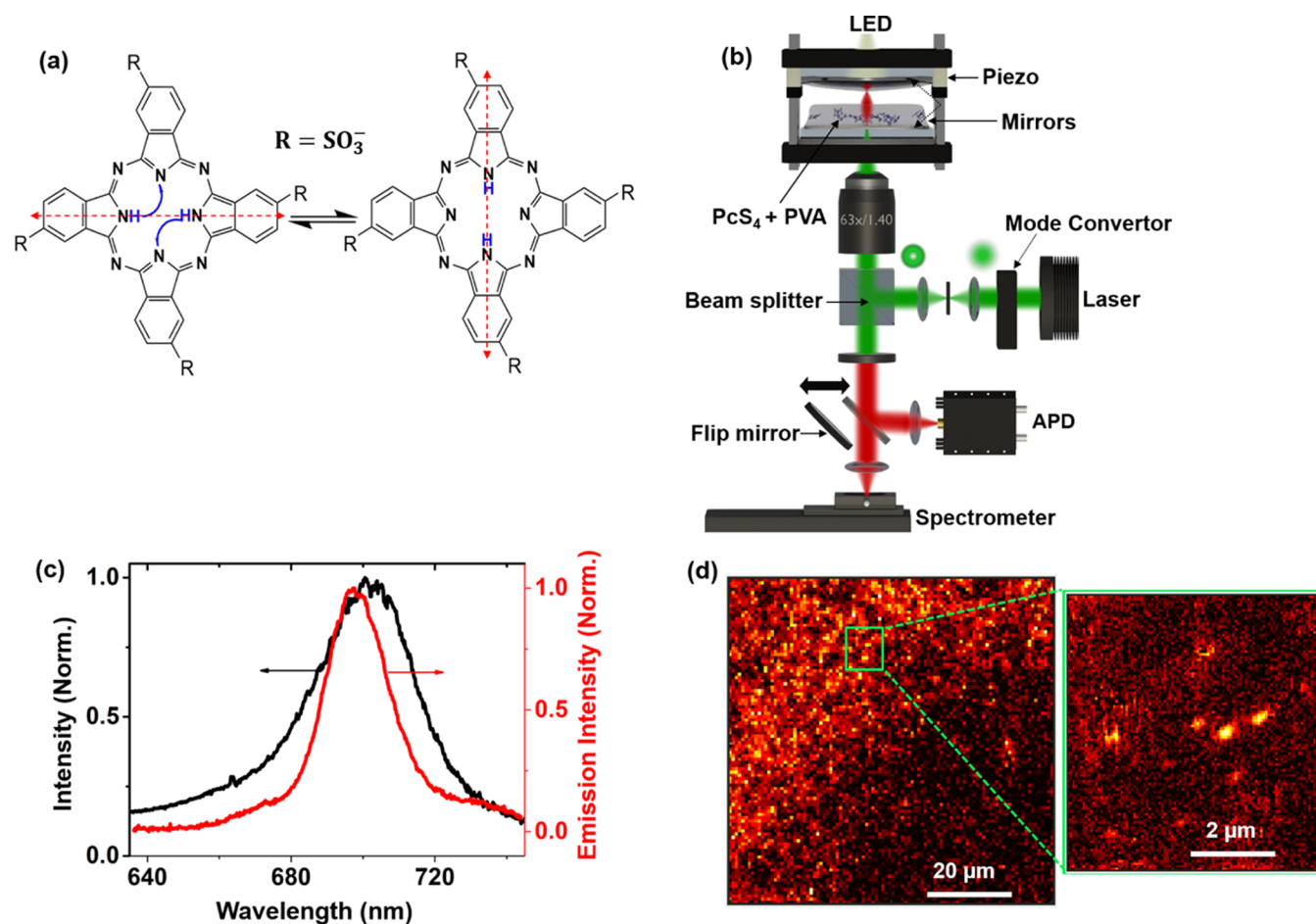
Figure 1. (a) Schematic of the tautomerization of phthalocyanine tetrasulfonate (PcS_4) by intramolecular double hydrogen transfer. The orientation of the transition dipole moment, as indicated by the red dashed arrow, rotates by 90° during tautomerization. (b) Schematic illustration of the piezotunable microcavity along with a simplified confocal microscope setup. (c) Exemplary microcavity transmission spectrum (black) and free space emission spectrum of a PcS_4–PVA film (red). The resonance condition was achieved by tuning the transmission maximum of the cavity toward the emission maximum of PcS_4. (d) Scanning confocal fluorescence microscopy image of the first-order interference region of the $\lambda/2$ microcavity with individual PcS_4 molecules embedded in a PVA film appearing as bright spots (acquired with a Gaussian-shaped laser).

spectral diffusion,[32] follow the spectral changes for the NH tautomers at cryogenic temperatures,[33] and visualize vibrational normal modes with atomically confined light.[34] They have also been employed in plasmon-enhanced fluorescence spectroscopy.[35] During NH tautomerization in porphyrins and phthalocyanines, the switching happens without significant conformational change.[13] It has been proposed to use this intriguing property in the single-molecule-based "hardware" elements such as molecular switches[13] and photonic molecular wires.[36] The application of porphyrin and phthalocyanine derivatives in functional molecular switches has been reviewed by Martynov et al.[37] In free-base Pcs, the orientation of the transition dipole moment (TDM) rotates by 90° upon tautomerization,[5,6] which can directly be visualized by the combination of confocal microscopy with cylindrical vector beams.[4–7] In this work, we show that reducing the residence time of a molecule in the singlet excited state via the Purcell effect has a significant influence on tautomerization, which is monitored via reorientation of the TDM.

■ METHODS

Phthalocyanine tetrasulfonate (PcS_4) and poly(vinyl alcohol) (PVA) were purchased from Sigma-Aldrich and used without further purification. Microscopy coverslips were cleaned with a chromosulfuric acid solution and rinsed with triply distilled water and spectroscopic-grade methanol (Uvasol, Merck, Germany).

Optical Microcavity Preparation. The microcavity structure used in these experiments is based on the tunable cavity structure originally designed by Meixner and co-workers.[38,39] It consists of two silver mirrors. The bottom mirror was prepared by sequentially evaporating 0.5 nm Cr, 30 nm Ag, and 70 nm SiO_2 layers on a clean microscope coverslip, while the top cavity mirror was prepared on a convex lens by covering it with 0.5 nm Cr, 60 nm Ag, and 70 nm SiO_2 layers, consecutively. The metal and dielectric layers were prepared using electron-beam evaporation (EB3, Edwards) under a high vacuum condition ($p \approx 10^{-6}$ mbar). The layer thickness was controlled during the evaporation process with an oscillating quartz unit (FTM7, Edwards). The Cr layer was used for adhesion, while the SiO_2 layer prevented the contact between the embedded dye molecules and the Ag film to prevent fluorescence quenching. The final microcavity structure was assembled by gluing the lower and the upper mirror onto a home-built mirror holder. A piezoactuator kinematic mirror mount (KC1-PZ/M, Thorlabs) was used to tune the cavity length by moving the upper mirror relative to the fixed-bottom
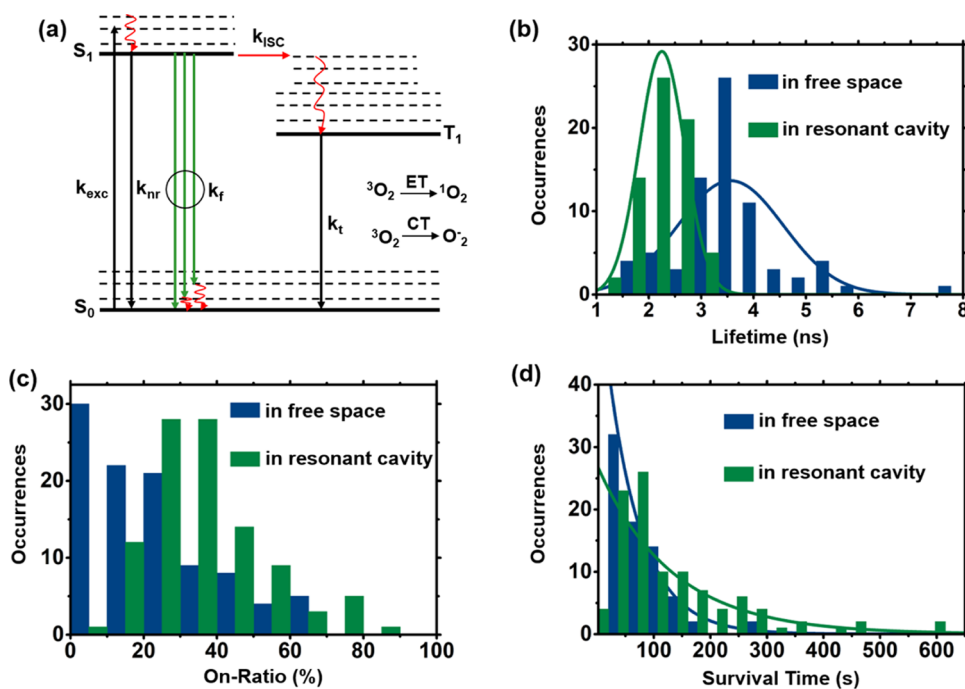
Figure 2. (a) Simplified Jabłoński scheme showing the effect of an optical field in a microcavity on the excitation/emission and the switching of a single molecule between fluorescent (ON) and dark (OFF) states and photobleaching. The rate constants k_{exc}, k_f, k_{isc}, and k_t refer to the excitation, fluorescence, S_1-T_1 intersystem crossing, and triplet decay rates, respectively. (b) Single-molecule fluorescence lifetime distributions of PcS_4 molecules in free space ($n = 74$, blue) and in the resonant microcavity ($n = 68$, green). The solid lines are normal distribution fits to the histograms. (c) On-ratio histogram for single PcS_4 molecules embedded in PVA in free space and inside the resonant microcavity. (d) Survival times histogram of single PcS_4 molecules. The solid lines show exponential fits to the histograms obtained from molecules embedded in the PVA matrix in free space and placed inside a microcavity, respectively.

mirror. For all measurements, the optical path length was adjusted to be in the first cavity order ($L_{op} = \lambda/2$).

Optical Measurements. For recording ensemble optical absorption and fluorescence emission spectra, PcS_4 was dissolved in water and diluted to a concentration of 10^{-6} M. The ensemble optical absorption spectrum was measured with a UV−vis spectrophotometer (Shimadzu UV-2700). The ensemble fluorescence measurements were recorded with a home-built confocal microscope, using a spin-coated sample (10^{-6} M PcS_4 and 2% w/v PVA in water) on the coverslip at the speed of 4000 rpm.

For all single-molecule investigations, a solution of PVA (1% w/v) and PcS_4 (10^{-9} M) in water was spin-coated on clean coverslips or on the lower mirror of the cavity at speeds of 8000 rpm. Single-molecule imaging, time trace, photon antibunching, and lifetime measurements were recorded using a home-built confocal microscope. For excitation, either a continuous wave at 633 nm (5 μW) or a pulsed laser at 640 nm (5 μW, pulse length 100 ns, repetition rate 10 MHz) was used. The collimated excitation beam was focused onto the sample with a high numerical aperture oil objective lens (Carl Zeiss, NA = 1.46). The fluorescence emission was collected by the same objective lens and separated from reflected laser light by appropriate long-pass filters. By raster scanning the sample through the diffraction-limited focal spot, confocal fluorescence images were recorded using an avalanche photodiode (APD). For the spectral measurements, a spectrograph (SP-2500i, Princeton Instruments) equipped with a charge-coupled device (CCD) camera (ProEM:512B+, Princeton Instruments) was used.

For photon antibunching measurements, the fluorescence signal was split by a 50:50 nonpolarizing beam splitter and

focused onto two APDs. The photons impinging on the detectors were detected by a time-correlated single-photon counting system (TCSPC, HydraHarp 400, PicoQuant). These data were plotted as a histogram of the time differences between the photons at both detectors showing photon antibunching, which was analyzed with SymPhoTime 64. Both continuous-wave and pulsed excitations were used for photon antibunching measurements (Figure S1b). Time-resolved fluorescence decay curves were recorded by TCSPC with a pulsed laser ($\lambda_{ex} = 640$ nm). The fluorescence lifetime decay curves were analyzed and fitted with SymPhoTime 64.

For imaging of tautomerization in PcS_4, azimuthally and radially polarized doughnut modes (APDM and RDPM) were used for excitation. The higher-order laser modes were generated by propagating the Gaussian-shaped beam of the 633 nm laser through a commercial mode converter (Arcoptix). The electric field distribution of the APDM allows imaging of the orientation of the transition dipole moment projected in the sample plane, while the RPDM enables the determination of both in-plane and out-of-plane components of the transition dipole moment (Figure S4).[5,40,41] The resulting image patterns reflect the orientation of the transition dipole moment, and the tautomerization of the single PcS_4 molecule can be directly observed via the change of the pattern.[4−7]

■ RESULTS AND DISCUSSION

Tautomerization of phthalocyanine tetrasulfonate (PcS_4) by intramolecular double hydrogen transfer is schematically shown in Figure 1a. The optical microcavity is illustrated in Figure 1b together with a simplified sketch of the confocal
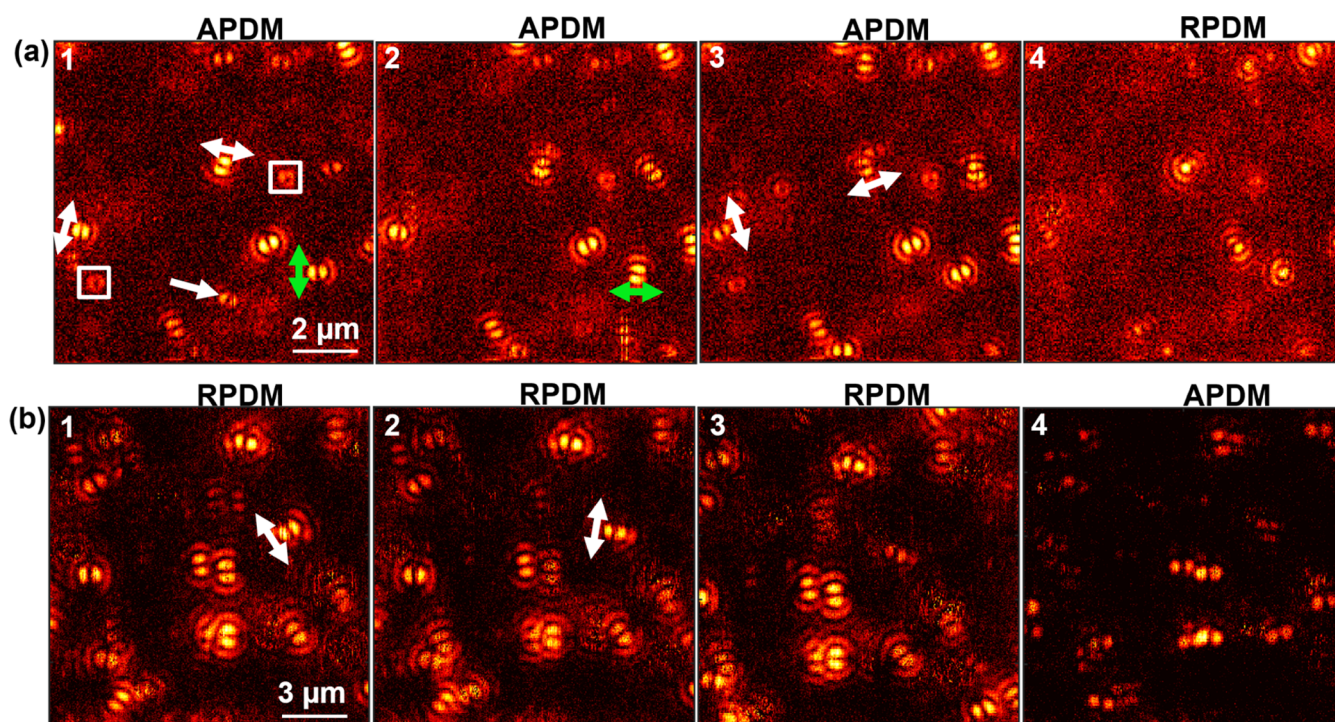
Figure 3. Impact of the Purcell effect on the tautomerization of individual PcS$_4$ molecules. Series of confocal fluorescence images of single PcS$_4$ molecules embedded in PVA acquired with azimuthal (APDM) and radial (RPDM) polarizations in free space (a) and in a $\lambda/2$ microcavity (b). Molecules that show double-lobe patterns and a reorientation of the transition dipole moment are marked with double-headed arrows, whereas white rectangles mark those that show ringlike patterns. For the molecule marked by the green double arrow, the orientation of the transition dipole moment rotates by 90° in the course of tautomerization.

microscope setup (for details, see Methods). The transmission spectrum of an empty microcavity, recorded when the microcavity is illuminated from above with a white-light-emitting diode (LED), is shown in Figure 1c. The transmission maximum can be spectrally voltage-tuned toward the fluorescence emission maximum of PcS$_4$ (red curve in Figure 1c). A single-molecule fluorescence image obtained by raster scanning the PcS$_4$–PVA film inside the microcavity through the excitation focus is presented in Figure 1d. In the $\lambda/2$ microcavity, the emission occurs in a ring area where the molecular fluorescence matches the resonance condition of the microcavity (Figure 1d).[38,39,42] Antibunching data obtained from isolated fluorescent spots confirm that individual PcS$_4$ molecules are observed inside the microcavity (Figures S1 and S2a).

Figure 2a shows a simplified Jabłoński diagram, where the solid and dashed horizontal black lines represent the electronic and vibrational energy levels of the molecule, respectively. Single molecules are excited from the lowest vibrational level of the electronic ground state (S$_0$) into a higher vibrational energy level of the first electronically excited state (S$_1$).[43] The radiative decay into a vibrational level of S$_0$, associated with the emission of a fluorescence photon, is indicated by green arrows with the rate constant k_f, which can be influenced by the microcavity.

A representative time-correlated single-photon counting decay for a molecule in a PVA matrix (blue line) and another molecule in a PVA matrix enclosed in a resonant microcavity (green line) is shown in Figure S2b. Single exponential fits to the fluorescence decays give fluorescence lifetimes of 3.58 and 2.31 ns for these particular molecules embedded in a thin PVA film in free space and inside a resonant microcavity,

respectively. The errors, i.e., the width of the 95% margin for both representative decays, are 0.04 ns. Figure 2b displays the fluorescence lifetime distribution of n single PcS$_4$ molecules embedded in PVA film ($n = 74$) in free space and inside the resonant microcavity ($n = 68$). Average fluorescence lifetimes are obtained by fitting the histograms with a normal distribution function. For molecules embedded in PVA, the average lifetime is 3.56 ns with a distribution width of 1.01 ns, while inside the resonant microcavity, the average lifetime decreases to 2.25 ns with a distribution width of 0.43 ns. The widths of the single-molecule fluorescence lifetime distributions presented in Figure 2b are significantly larger than the 95% confidence intervals from fitting the decay curves. The dielectric environment can have a significant influence on the fluorescence lifetime distribution due to local fluctuations of the refractive index.[44,45] Hence, the width of the lifetime distribution is not caused by statistical fluctuations, but reflects the heterogeneity of the local environments.

An alternative pathway to radiative deactivation is the intersystem crossing from S$_1$ to the long-lived triplet state T$_1$, which gives rise to nonemissive dark (OFF) states, causing intermittent fluorescence emission (blinking). Representative fluorescence intensity time traces of single PcS$_4$ molecules are shown in Figure S2c,d. For molecules embedded in PVA in free space, the ON and OFF states appear with several long OFF time periods (Figure S2c), while in the resonant microcavity, the OFF states are not observed for extended periods of time (Figure S2d). This shows qualitatively that the reduction of the excited state lifetime by the microcavity has an influence on the blinking dynamics of single PcS$_4$ molecules. A measure of this change in the blinking dynamics is the ON ratio K_{on}, which can be calculated from the intensity time

traces by $K_{on} = \left(\frac{t_{on}}{t_{on} + t_{off}}\right) \times 100.$[46] The ON ($t_{on}$) and OFF times ($t_{off}$) of a molecule can be determined from such intensity trajectories by defining a threshold, indicated by the black dashed line in Figure S2c,d, as twice the background signal for a molecule that is in the bright state. We have calculated K_{on} for a population of 102 PcS$_4$ molecules embedded in the PVA matrix and 102 placed inside a $\lambda/2$ microcavity (Figure 2c). For the sample embedded in PVA in free space, the average ON ratio is 23%, whereas for the molecules placed inside the resonant microcavity, the average ON ratio increases to 36%. This confirms that the microcavity reduces the possibility of a molecule entering into the nonfluorescent triplet state by decreasing the residence time of the molecule in the S$_1$ state. Additionally, the reactivity of the triplet state with atmospheric triplet oxygen ($^3O_2$) can lead to permanent damage of the fluorophore (photobleaching) by the creation of highly unstable species, such as singlet oxygen ($^1O_2$) or superoxide radical (O_2^-).[47,48] The survival time, which is defined as the total time before a single molecule undergoes irreversible photobleaching, can also be influenced by the microcavity. The survival time distributions for single PcS$_4$ molecules embedded in PVA in free space ($n = 102$) and placed inside a resonant microcavity ($n = 102$) are shown in Figure 2d. Fitting the distributions with single exponential decay functions gives mean survival times of 61.39 ± 14.28 and 142.53 ± 55.82 s for the molecules embedded in PVA in free space and in the resonant cavity, respectively. The errors are calculated by considering the 95% confidence interval of the fitting parameter of the exponential decay function.

To unveil the relation between the fluorescence emission changes due to the Purcell effect and the rate of the tautomerization reaction, a series of consecutive fluorescence images were recorded for single PcS$_4$ molecules embedded in a PVA film (in free space) and inside the resonant cavity (Figure 3). For samples embedded in PVA, the molecules excited with azimuthal polarization doughnut mode (APDM) have either a ringlike or a double-lobe pattern shape. A ringlike pattern shape indicates that multiple tautomerizations did occur during the acquisition of the pattern, while a double-lobe pattern is obtained for a fixed TDM, i.e., localization of the inner hydrogens. For example, among the 11 single molecules observed in the image shown in Figure 3a panel, (1) two single molecules show ringlike patterns, as indicated by the white rectangles, and nine show double-lobe patterns. More examples are given in Figure S3. The molecule indicated by the white arrow bleaches after one scan. The single molecules marked with two-headed arrows show a sudden reorientation of the double-lobe pattern in consecutive scans. Since the PcS$_4$ molecules are embedded in a PVA matrix, molecular rotation can be excluded and the reorientation of the double-lobe pattern must be attributed to different directions of the TDM of the same PcS$_4$ molecule due to tautomerization. Additionally, the full three-dimensional (3D) orientation of the molecules can be determined with the radially polarized doughnut mode (RPDM), since it has both in-plane and longitudinal polarization components and molecules excited with the RPDM show both spotlike and double-lobe patterns (Figure 3a, panel 4).[5]

The observed brightness of the individual image patterns strongly depends on the orientation of the transition dipole moment relative to the excitation field. For example, the APDM is exclusively polarized in the sample plane, and

molecules lying in this plane will appear brightest, whereas any tilt out of the image plane will reduce the excitation efficiency and consequently the intensity of the detected signal. However, in the case of the APDM, such a tilt does not have an influence on the pattern shape but only on the intensity. The intensity distribution of the electric field component in the focus of the APDM and the RPDM is shown in Figure S4. Additionally, the brightness of the individual images strongly depends on the local environment surrounding the molecule. As shown in Figure 2, the average fluorescence lifetime varies significantly between the molecules, leading to a different number of photons emitted within a certain time period. The observed overlapping of the fluorescence patterns occurs due to molecules being close to each other but still separated by distances larger than the diffraction limit (>200 nm). The fluorescence images display different characteristics; for instance, the appearance of partial patterns. Incomplete fluorescence patterns occur due to (i) transitions to a dark state (usually causing stripes in the image pattern) and (ii) photobleaching of the molecule.

Consecutive fluorescence images of single PcS$_4$ molecules inside the resonant microcavity are shown in Figure 3b. All of them show double-lobe patterns regardless of the excitation mode, since focusing a laser beam into a microcavity changes the field distribution with respect to the free space focus. Khoptyar et al.[49] demonstrated that the in-plane components of the RPDM and the APDM have their field intensity maximum in the center of the cavity and zero intensity at the cavity mirrors, while the longitudinal component of RPDM has a maximum at the cavity mirrors and a minimum in the center (see Figure S4). All measurements were conducted in the $\lambda/2$ region of the cavity and the molecules are located close to the center of the cavity, hence they are only excited by the in-plane component of both the RPDM and APDM, which results in a double-lobe pattern for both excitation modes. In Figure 3b (1), 13 single molecules can be observed and only one shows a reorientation of the TDM.

A strict 90° rotation of the image pattern can only be observed for molecules with a transition dipole moment oriented strictly perpendicular to the optical axis of the microscope, e.g., molecules lying flat on a glass substrate.[6] The molecules in this work are randomly oriented within the polymer layer, and any tilt of the transition dipole moment out of the image plane alters the observed flipping angle. The orientation of the image pattern acquired with the APDM depends exclusively on the projection of the transition dipole moment on the image plane. Hence, the observed flipping angle will, in the majority of cases, deviate from 90°. Consequently, we have observed 90° flipping only for a few molecules; for instance, the molecule marked by the green double arrow shown in Figure 3a.

For statistical analysis, the observed single-molecule patterns are classified into three categories: double-lobe not flipped, double-lobe flipped, and ringlike patterns. The histogram presenting the relative contributions of these three pattern shapes is shown in Figure 4. For PcS$_4$ molecules embedded in PVA in free space, 22% from a population of 110 single molecules exhibit a reorientation of the TDM. In 8% of the molecules, a ringlike pattern is observed. On the other hand, 94% of single molecules ($n = 110$) inside a resonant microcavity exhibit a stable TDM orientation, and only 6% of the molecules show reorientation of the TDM during consecutive scans. This confirms that the Purcell effect can be
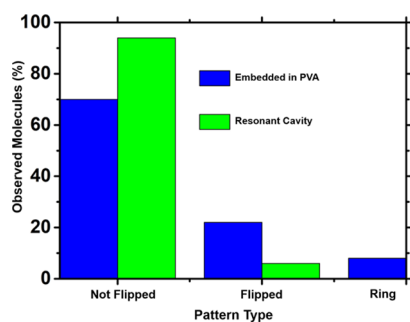
Figure 4. Comparing the occurrence of different fluorescence excitation patterns associated with tautomerization of a fraction of single molecules (n = 110) that show double-lobe and ringlike patterns in free space (blue) and inside a resonant $\lambda/2$ microcavity (green).

used to alter the tautomerization properties of single molecules.

To understand the mechanisms responsible for reduced tautomerization probability observed for phthalocyanine molecules in a resonant optical microcavity, we start by recalling the current knowledge about tautomerization in structurally similar systems, porphyrins.[17,18] In porphyrin, this reaction occurs in the ground electronic state on the time scale of tens of microseconds at room temperature.[21] The transfer is stepwise: first, a single hydrogen transfer leads to a higher energy cis tautomer, which then undergoes a second transfer, either a back reaction to the initial trans form or a chemically equivalent trans structure with two hydrogen atoms transferred. The trans–cis conversion involves tunneling from an excited vibrational level, which can be populated by thermal activation. Therefore, ground-state tautomerization stops at low temperatures, practically below 100 K. However, even at helium temperature, tautomerization can be induced using light.[50−52] The exact mechanism is still unknown; it has been proposed that the process occurs from the lowest triplet state,[50] although the involvement of "vibrationally hot" ground electronic state could not be excluded.

Structurally, phthalocyanines are similar to porphyrins,[20,53−55] regarding the H-bond parameters, as can be deduced from very similar values of the NH stretching frequencies.[53] Therefore, similar tautomerization mechanisms can be expected, and the work of Strenalyuk et al.[20] confirmed this assumption. A comparative single-molecule spectroscopic study of porphyrin and porphyrazine-like molecules indicates that tautomerization occurs during vibronic relaxation in the first electronically excited state, particularly in those cases where fast tautomerization is locked due to the interaction with the local environment.[5] This was also confirmed in a recent study of single free-base phthalocyanine molecules by combined STM-fluorescence methodology, the experiment indicated that the excited state is involved in the tautomerization path.[3] Even though the authors did not specifically mention which electronic state is involved, it seems that the triplet route is the most plausible one. The quantum yield of tautomerization (ϕ_{taut}) occurring in the triplet state is given by $\phi_{taut} = \phi_T \cdot k_r \cdot \tau_T$, where ϕ_T is the triplet formation yield, k_r is the tautomerization rate, and τ_T is the triplet lifetime. The triplet formation yield $\phi_T = k_{ISC} \cdot \tau_s$ does depend on the intersystem crossing rate k_{ISC} and the singlet excited state lifetime τ_s. As discussed above, the lifetime τ_s (Figure 2b) is reduced in resonant microcavity leading to a reduction of ϕ_T, which is

observed by a reduction of blinking and photobleaching (Figure 2c,d). As a consequence, also tautomerization is less likely, which is clearly observed in Figure 4. However, one may wonder whether the decrease in the fluorescence lifetime by a factor of 2 is sufficient to lower the tautomerization yield to the extent observed in Figure 4. A reduction of τ_T cannot be the reason for a lower ϕ_{taut}, since it is not influenced by the cavity. However, another possible source of a lower ϕ_{taut} might be a change in the tautomerization potential in the triplet state, which would lead to a decrease of k_r.

Another observation that should be explained is the apparent lack of ground-state tautomerization for molecules in the cavity. While the ground-state conversion should take place in microseconds, it seems unlikely that the tautomerization rate for the molecule in the ground state is affected by the optical mode density in the microcavity. We note that in a single-molecule fluorescence experiment, the molecule continuously cycles between S_0, S_1, and T_1. As soon as the molecule returns to S_0, it is immediately excited again, which leaves no time for ground-state tautomerization. Such a situation is completely different from the case of molecular ensembles, where, for usually applied concentration and excitation power, a molecule absorbs, on average, about one photon per second. Therefore, a single-molecule experiment is in fact probing tautomerization in the longest-lived state, the triplet.

CONCLUSIONS

Tautomerization is a reversible chemical reaction that may result in chemically identical species and does not involve a conformational change. Because of these intriguing properties, tautomerization reactions have been proposed to act as molecular switches. Thus, finding a "'physical'" method of manipulating tautomerization, and other intramolecular reactions, is crucial to design and control molecular optoelectronics.[13,14] Here, we have investigated the influence of the Purcell effect on the tautomerization of single molecules at room temperature by placing single PcS4 molecules inside an optical $\lambda/2$ microcavity. Molecules on resonance with the microcavity mode have a shorter fluorescence lifetime, and the excited singlet state is depopulated faster; as a consequence, the transition rate to the triplet state is reduced. As a result, we observed that the molecules in a resonant cavity stay locked in a specific tautomeric form for a longer time since the lowest triplet state is less frequently populated. This suggests that in our single-molecule method, we probe tautomerization reactions in the lowest triplet state. It is thus feasible that by modulating the coupling between an individual molecule and a cavity structure, the intramolecular reactions could be switched on and off at will. Furthermore, our findings indicate that weak coupling between the cavity mode and molecular transition can be used to limit the damage of an excited molecule by reactive oxygen and to steer excited-state photoinduced chemical processes toward the desired direction.

ASSOCIATED CONTENT

SI Supporting Information

The Supporting Information is available free of charge at https://pubs.acs.org/doi/10.1021/acs.jpcc.1c02600.

> Methods, a fluorescence image of single PcS4 molecule embedded in PVA in free space, single PcS4 molecule photon antibunching results, time-correlated single-photon counting decay traces, fluorescence intensity

time trace, confocal fluorescence images of single PcS$_4$ molecules embedded in PVA acquired with APDM and RPDM polarization in free space and a resonant $\lambda/2$ microcavity, and comparison of the field intensity distribution of the APDM and the RPDM in free space and $\lambda/2$ microcavity (PDF)

AUTHOR INFORMATION

Corresponding Authors

Frank Wackenhut − *Institute of Physical and Theoretical Chemistry, University of Tübingen, D-72076 Tübingen, Germany;* orcid.org/0000-0001-6554-6600; Email: frank.wackenhut@uni-tuebingen.de

Lukasz Piatkowski − *Faculty of Materials Engineering and Technical Physics, Poznań University of Technology, 60-965 Poznań, Poland;* orcid.org/0000-0002-1226-2257; Email: lukasz.j.piatkowski@put.poznan.pl

Alfred J. Meixner − *Institute of Physical and Theoretical Chemistry, University of Tübingen, D-72076 Tübingen, Germany;* orcid.org/0000-0002-0187-2906; Email: alfred.meixner@uni-tuebingen.de

Authors

Wassie Mersha Takele − *Institute of Physical and Theoretical Chemistry, University of Tübingen, D-72076 Tübingen, Germany; Institute of Physical Chemistry, Polish Academy of Sciences, 01-224 Warsaw, Poland*

Quan Liu − *Institute of Physical and Theoretical Chemistry, University of Tübingen, D-72076 Tübingen, Germany; Laboratoire Lumière, nanomatériaux and nanotechnologies—L2n and CNRS ERL 7004, Université de Technologie de Troyes, 10000 Troyes, France*

Jacek Waluk − *Institute of Physical Chemistry, Polish Academy of Sciences, 01-224 Warsaw, Poland; Faculty of Mathematics and Science, Cardinal Stefan Wyszyński University, 01-815 Warsaw, Poland*

Complete contact information is available at:
https://pubs.acs.org/10.1021/acs.jpcc.1c02600

Notes

The authors declare no competing financial interest.

REFERENCES

(1) Claramunt, R. M.; Lopez, C.; Santa Maria, M. D.; Sanz, D.; Elguero, J. The Use of NMR Spectroscopy to Study Tautomerism. *Prog. Nucl. Magn. Reson. Spectrosc.* **2006**, *49*, 169−206.

(2) Fita, P.; Grill, L.; Listkowski, A.; Piwoński, H.; Gawinkowski, S.; Pszona, M.; Sepioł, J.; Mengesha, E.; Kumagai, T.; Waluk, J. Spectroscopic and Microscopic Investigations of Tautomerization in Porphycenes: Condensed Phases, Supersonic Jets, and Single Molecule Studies. *Phys. Chem. Chem. Phys.* **2017**, *19*, 4921−4937.

(3) Doppagne, B.; Neuman, T.; Soria-Martinez, R.; López, L. E. P.; Bulou, H.; Romeo, M.; Berciaud, S.; Scheurer, F.; Aizpurua, J.; Schull, G. Single-Molecule Tautomerization Tracking through Space- and Time-Resolved Fluorescence Spectroscopy. *Nat. Nanotechnol.* **2020**, *15*, 207−211.

(4) Piwoński, H.; Stupperich, C.; Hartschuh, A.; Sepioł, J.; Meixner, A.; Waluk, J. Imaging of Tautomerism in a Single Molecule. *J. Am. Chem. Soc.* **2005**, *127*, 5302−5303.

(5) Chizhik, A. M.; Jäger, R.; Chizhik, A. I.; Bär, S.; MacK, H. G.; Sackrow, M.; Stanciu, C.; Lyubimtsev, A.; Hanack, M.; Meixner, A. J. Optical Imaging of Excited-State Tautomerization in Single Molecules. *Phys. Chem. Chem. Phys.* **2011**, *13*, 1722−1733.

(6) Ikeda, T.; Iino, R.; Noji, H. Real-Time Fluorescence Visualization of Slow Tautomerization of Single Free-Base Phthalocyanines under Ambient Conditions. *Chem. Commun.* **2014**, *50*, 9443−9446.

(7) Piatkowski, L.; Schanbacher, C.; Wackenhut, F.; Jamrozik, A.; Meixner, A. J.; Waluk, J. Nature of Large Temporal Fluctuations of Hydrogen Transfer Rates in Single Molecules. *J. Phys. Chem. Lett.* **2018**, *9*, 1211−1215.

(8) Kumagai, T.; Hanke, F.; Gawinkowski, S.; Sharp, J.; Kotsis, K.; Waluk, J.; Persson, M.; Grill, L. Controlling Intramolecular Hydrogen Transfer in a Porphycene Molecule with Single Atoms or Molecules Located Nearby. *Nat. Chem.* **2014**, *6*, 41−46.

(9) Sperl, A.; Kröger, J.; Berndt, R. Controlled Metalation of a Single Adsorbed Phthalocyanine. *Angew. Chem., Int. Ed.* **2011**, *50*, 5294−5297.

(10) Böckmann, H.; Liu, S.; Mielke, J.; Gawinkowski, S.; Waluk, J.; Grill, L.; Wolf, M.; Kumagai, T. Direct Observation of Photoinduced Tautomerization in Single Molecules at a Metal Surface. *Nano Lett.* **2016**, *16*, 1034−1041.

(11) Ladenthin, J. N.; Frederiksen, T.; Persson, M.; Sharp, J. C.; Gawinkowski, S.; Waluk, J.; Kumagai, T. Force-Induced Tautomerization in a Single Molecule. *Nat. Chem.* **2016**, *8*, 935−940.

(12) Kügel, J.; Leisegang, M.; Böhme, M.; Krönlein, A.; Sixta, A.; Bode, M. Remote Single-Molecule Switching: Identification and Nanoengineering of Hot Electron-Induced Tautomerization. *Nano Lett.* **2017**, *17*, 5106−5112.

(13) Liljeroth, P.; Repp, J.; Meyer, G. Current-Induced Hydrogen. Current-Induced Hydrogen Tautomerization and Conductance Switching of Naphthalocyanine Molecules. *Science* **2007**, *317*, 1203−1206.

(14) Mangel, S.; Skripnik, M.; Polyudov, K.; Dette, C.; Wollandt, T.; Punke, P.; Li, D.; Urcuyo, R.; Pauly, F.; Jung, S. J.; Kern, K. Electric-Field Control of Single-Molecule Tautomerization. *Phys. Chem. Chem. Phys.* **2020**, *22*, 6370−6375.

(15) Srivastava, R. The Role of Proton Transfer on Mutations. *Front. Chem.* **2019**, *7*, No. 536.

(16) Taylor, P. J.; van der Zwan, G.; Antonov, L. Tautomerism: Introduction, History, and Recent Developments in Experimental and Theoretical Methods. *Tautomerism: Methods and Theories*; Wiley-VCH Verlag GmbH, 2013; pp 1−24.

(17) Maity, D. K.; Truong, T. N. Status of Theoretical Modeling of Tautomerization in Free-Base Porphyrin. *J. Porphyrins Phthalocyanines* **2001**, *5*, 289−299.

(18) Waluk, J. Spectroscopy and Tautomerization Studies of Porphycenes. *Chem. Rev.* **2017**, *117*, 2447−2480.

(19) Nemykin, V. N.; Sabin, J. R. Profiling Energetics and Spectroscopic Signatures in Prototropic Tautomers of Asymmetric Phthalocyanine Analogues. *J. Phys. Chem. A* **2012**, *116*, 7364−7371.

(20) Strenalyuk, T.; Samdal, S.; Volden, H. V. Molecular Structure of Phthalocyaninatotin(II) Studied by Gas-Phase Electron Diffraction and High-Level Quantum Chemical Calculations. *J. Phys. Chem. A* **2008**, *112*, 10046−10052.

(21) Braun, J.; Limbach, H. H.; Schlabach, M.; Wehrle, B.; Köcher, M.; Vogel, E. NMR Study of the Tautomerism of Porphyrin Including the Kinetic HH/HD/DD Isotope Effects in the Liquid and the Solid State. *J. Am. Chem. Soc.* **1994**, *116*, 6593−6604.

(22) Fita, P.; Urbańska, N.; Radzewicz, C.; Waluk, J. Ground-and Excited-State Tautomerization Rates in Porphycenes. *Chem. − Eur. J.* **2009**, *15*, 4851−4856.

(23) Pelton, M. Modified Spontaneous Emission in Nanophotonic Structures. *Nat. Photonics* **2015**, *9*, 427−435.

(24) Cang, H.; Liu, Y.; Wang, Y.; Yin, X.; Zhang, X. Giant Suppression of Photobleaching for Single Molecule Detection via the Purcell Effect. *Nano Lett.* **2013**, *13*, 5949−5953.

(25) Wientjes, E.; Renger, J.; Curto, A. G.; Cogdell, R.; Van Hulst, N. F. Strong Antenna-Enhanced Fluorescence of a Single Light-Harvesting Complex Shows Photon Antibunching. *Nat. Commun.* **2014**, *5*, No. 4236.

(26) Schleifenbaum, F.; Kern, A. M.; Konrad, A.; Meixner, A. J. Dynamic Control of Förster Energy Transfer in a Photonic Environment. *Phys. Chem. Chem. Phys.* **2014**, *16*, 12812−12817.

(27) Konrad, A.; Metzger, M.; Kern, A. M.; Brecht, M.; Meixner, A. J. Controlling the Dynamics of Förster Resonance Energy Transfer inside a Tunable Sub-Wavelength Fabry-Pérot-Resonator. *Nanoscale* **2015**, *7*, 10204−10209.

(28) Stefani, F. D.; Vasilev, K.; Bocchio, N.; Gaul, F.; Pomozzi, A.; Kreiter, M. Photonic Mode Density Effects on Single-Molecule Fluorescence Blinking. *New J. Phys.* **2007**, *9*, 21.

(29) Howe, L.; Zhang, J. Z. Ultrafast Studies of Excited-State Dynamics of Phthalocyanine and Zinc Phthalocyanine Tetrasulfonate in Solutions. *J. Phys. Chem. A* **1997**, *101*, 3207−3213.

(30) Paulo, P. M. R.; Costa, S. M. B. Single-Molecule Fluorescence of a Phthalocyanine in Pamam Dendrimers Reveals Intensity-Lifetime Fluctuations from Quenching Dynamics. *J. Phys. Chem. C* **2010**, *114*, 19035−19043.

(31) Yang, B.; Chen, G.; Ghafoor, A.; Zhang, Y.; Zhang, Y.; Zhang, Y.; Luo, Y.; Yang, J.; Sandoghdar, V.; Aizpurua, J.; Dong, Z.; Hou, J. G. Sub-Nanometre Resolution in Single-Molecule Photoluminescence Imaging. *Nat. Photonics* **2020**, *14*, 693−699.

(32) Savostianov, A. O.; Eremchev, I. Y.; Gorshelev, A. A.; Naumov, A. V.; Starukhin, A. S. Wide-Range Spectral Diffusion in Single Mg-Tetraazaporphyrin Molecules in a Polymer Matrix at Cryogenic Temperatures. *JETP Lett.* **2018**, *107*, 406−411.

(33) Starukhin, A.; Shulga, A.; Wild, U. P. Single-Site Spectra of NH-Tautomers of Nonsymmetrical Tetraethylporphyrins in an n-Octane Matrix at 10K. *J. Lumin.* **2001**, *93*, 81−92.

(34) Lee, J.; Crampton, K. T.; Tallarida, N.; Apkarian, V. A. Visualizing vibrational normal modes of a single molecule with atomically confined light. *Nature* **2019**, *568*, 78−82.

(35) Francisco, A. P.; Botequim, D.; Prazeres, D. M. F.; Serra, V. V.; Costa, S. M. B.; Laia, C. A. T.; Paulo, P. M. R. Extreme Enhancement of Single-Molecule Fluorescence from Porphyrins Induced by Gold Nanodimer Antennas. *J. Phys. Chem. Lett.* **2019**, *10*, 1542−1549.

(36) Abdel-Latif, M. K.; Kühn, O. Laser Control of Double Proton Transfer in Porphycenes: Towards an Ultrafast Switch for Photonic Molecular Wires. *Theor. Chem. Acc.* **2011**, *128*, 307−316.

(37) Martynov, A. G.; Safonova, E. A.; Tsivadze, A. Y.; Gorbunova, Y. G. Functional Molecular Switches Involving Tetrapyrrolic Macro-cycles. *Coord. Chem. Rev.* **2019**, *387*, 325−347.

(38) Chizhik, A.; Schleifenbaum, F.; Gutbrod, R.; Chizhik, A.; Khoptyar, D.; Meixner, A. J.; Enderlein, J. Tuning the Fluorescence Emission Spectra of a Single Molecule with a Variable Optical Subwavelength Metal Microcavity. *Phys. Rev. Lett.* **2009**, *102*, No. 073002.

(39) Bär, S.; Chizhik, A.; Gutbrod, R.; Schleifenbaum, F.; Chizhik, A.; Meixner, A. J. Microcavities: Tailoring the Optical Properties of Single Quantum Emitters. *Anal. Bioanal. Chem.* **2010**, *396*, 3−14.

(40) Züchner, T.; Failla, A. V.; Meixner, A. J. Light Microscopy with Doughnut Modes: A Concept to Detect, Characterize, and Manipulate Individual Nanoobjects. *Angew. Chem., Int. Ed.* **2011**, *50*, 5274−5293.

(41) Wackenhut, F.; Virgilio Failla, A.; Züchner, T.; Steiner, M.; Meixner, A. J. Three-Dimensional Photoluminescence Mapping and Emission Anisotropy of Single Gold Nanorods. *Appl. Phys. Lett.* **2012**, *100*, No. 263102.

(42) Steiner, M.; Schleifenbaum, F.; Stupperich, C.; Failla, A. V.; Hartschuh, A.; Meixner, A. J. Microcavity-Controlled Single-Molecule Fluorescence. *ChemPhysChem* **2005**, *6*, 2190−2196.

(43) Moerner, W. E.; Shechtman, Y.; Wang, Q. Single-Molecule Spectroscopy and Imaging over the Decades. *Faraday Discuss.* **2015**, *184*, 9−36.

(44) Naumov, A. V.; Gorshelev, A. A.; Gladush, M. G.; Anikushina, T. A.; Golovanova, A. V.; Köhler, J.; Kador, L. Micro-Refractometry and Local-Field Mapping with Single Molecules. *Nano Lett.* **2018**, *18*, 6129−6134.

(45) Aubret, A.; Orrit, M.; Kulzer, F. Understanding Local-Field Correction Factors in the Framework of the Onsager−Böttcher Model. *ChemPhysChem* **2019**, *20*, 345−355.

(46) Liu, Q.; Wackenhut, F.; Hauler, O.; Scholz, M.; Zur Oven-Krockhaus, S.; Ritz, R.; Adam, P. M.; Brecht, M.; Meixner, A. J. Hypericin: Single Molecule Spectroscopy of an Active Natural Drug. *J. Phys. Chem. A* **2020**, *124*, 2497−2504.

(47) Zheng, Q.; Juette, M. F.; Jockusch, S.; Wasserman, M. R.; Zhou, Z.; Altman, R. B.; Blanchard, S. C. Ultra-Stable Organic Fluorophores for Single-Molecule Research. *Chem. Soc. Rev.* **2014**, *43*, 1044−1056.

(48) Stennett, E. M. S.; Ciuba, M. A.; Levitus, M. Photophysical Processes in Single Molecule Organic Fluorescent Probes. *Chem. Soc. Rev.* **2014**, *43*, 1057−1075.

(49) Khoptyar, D.; Gutbrod, R.; Chizhik, A.; Enderlein, J.; Schleifenbaum, F.; Steiner, M.; Meixner, A. J. Tight Focusing of Laser Beams in a $\lambda/2$-Microcavity. *Opt. Express* **2008**, *16*, 9907.

(50) Völker, S.; Van Der Waals, J. H. Laser-Induced Photochemical Isomerization of Free Base Porphyrin in an n-Octane Crystal at 4-2 K. *Mol. Phys.* **1976**, *32*, 1703−1718.

(51) Radziszewski, J. G.; Waluk, J.; Michl, J. Site-Population Conserving and Site-Population Altering Photo-Orientation of Matrix-Isolated Freebase Porphine by Double Proton Transfer: IR Dichroism and Vibrational Symmetry Assignments. *Chem. Phys.* **1989**, *136*, 165−180.

(52) Radziszewski, J. G.; Waluk, J.; Michl, J. FT Visible Absorption Spectroscopy of Porphine in Noble Gas Matrices. *J. Mol. Spectrosc.* **1990**, *140*, 373−389.

(53) Stuzhin, P. A.; Khelevina, O. G. Azaporphyrins: Structure of the Reaction Centre and Reactions of Complex Formation. *Coord. Chem. Rev.* **1996**, *147*, 41−86.

(54) Martynov, A. G.; Mack, J.; Ngoy, B. P.; Nyokong, T.; Gorbunova, Y. G.; Tsivadze, A. Y. Electronic Structure and NH-Tautomerism of a Novel Metal-Free Phenanthroline-Annelated Phthalocyanine. *Dyes Pigm.* **2017**, *140*, 469−479.

(55) Wehrle, B.; Limbach, H.-h. NMR Study of Environment Modulated Proton Tautomerism in Crystalline and Amorphous Phthalocyanine. *Chem. Phys.* **1989**, *136*, 223−247.

H